Korean J. Chem. Eng., **25**(4), 663-669 (2008)

A continuous photocatalysis system in the degradation of herbicide

Nathaporn Areerachakul, Saravanamuthu Vigneswaran†, Huu Hao Ngo, and Jaya Kandasamy

Faculty of Engineering, University of Technology, Sydney, P.O. Box 123, Broadway, NSW 2007, Australia
(*Received 28 July 2007 • accepted 19 Ocober 2007*)

Abstract−The performance of both batch and continuous photo-catalytic reactors was studied to evaluate their capabilities in removing the sulfonyl urea herbicide of metsulfuron methyl (MM). It was found in a batch reactor that the addition of a small amount of powder activated carbon (PAC) significantly increased the rate of degradation of MM. The continuous photo-catalytic system resulted in 57% of MM removal. When a small dose of activated carbon was added in the photo-catalytic system, MM removal increased to 78-86% MM removal for retention times between of 5.25-21 min (corresponding to withdrawal rates of 10-40 $mLmin^{-1}$). In this study, the pseudo first order rate constants of a continuous photo-catalytic system revealed that shorter retention times were associated with lower rate constants. Solid phase micro extraction/gas chromatography (SPME/GC) results showed that high concentrations of MM were broken down to small volatile organic compounds (VOCs) by photo-catalytic oxidation. PAC adsorbed the photo-products and increased the degradation of MM.

Key words: Metsulfuron Methyl, Heterogeneous Photocatalysis, Powder Activated Carbon, Batch Photo-catalytic Reactor, Continuous Photo-catalytic Reactor

INTRODUCTION

Synthetic organic compounds (SOC) in water, which include most of the herbicides, are a major concern and cause health risks in the water supply. Advanced treatment processes such as powder activated carbon (PAC) adsorption, granular activated carbon (GAC) adsorption, and nanofiltration are highly effective in removing the herbicides. Nanofiltration can remove between 50-90% herbicides and pesticides from water containing low concentration of natural organic matters 0.4-3.6 mgL^{-1} [1]. PAC adsorption is effective in removing herbicides; however, it is expensive and does pose handling and disposal problems. Granular activated carbon (GAC) is an effective alternative to PAC and may be used in packed beds for the removal of herbicides.

Photo-catalytic oxidation is an alternative method for removing herbicide contaminants in water. Titanium dioxide (TiO_2), whhich is widely used as a photo-catalyst due to its low cost, is non-toxic and photo-chemically stable. This process is based on the electronic excitation of a molecule or solid caused by light absorption, e.g., UV light drastically alters its ability to lose or gain electrons and promote the decomposition of pollutants to harmless by-products [2]. Photo-induced electrons (e^-) and positive holes (h^+) are produced from TiO_2 in the presence of UV light (Eq. (1)). These charged species can further generate free radicals (Eqs. (2) and (3)). The highly oxidizing positive hole h^+ resulting from the TiO_2 photocatalysis is considered to be the dominant oxidizing species contributing to the mineralization process [3].

$$TiO_2 + h\nu \rightarrow TiO_2\,(e^- + h^+) \tag{1}$$

$$h^+ + OH^- \rightarrow HO\cdot \tag{2}$$

$$e^- + O_2 \rightarrow \cdot O_2 \tag{3}$$

†To whom correspondence should be addressed.
E-mail: s.vigneswaran@uts.edu.au

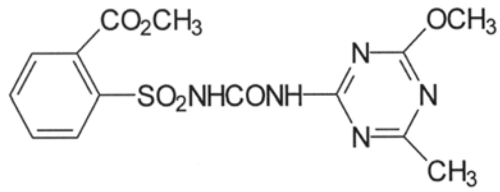

Fig. 1. The structure of Metsulfuron-methyl (MM).

In this study, the photo-catalytic oxidation process of metsulfuron methyl (MM) was investigated in the presence of TiO_2 and UV light. MM ($C_{14}H_{15}N_5O_6S$) is a widely used group B herbicide in Australia. The structure of MM is shown in Fig. 1.

EXPERIMENTAL SET-UP

The photocatalysis experiments were conducted by using batch and continuous photo-reactors.

1. Batch Reactor

The batch reactor used was equipped with three 8 W UV lamps, air blower, and magnetic bar (Fig. 2). The total surface area of the three lamps was 537 cm^2 and the volume of the reactor was 1.5 L. Air sparging was provided to supply oxygen into the reactor (3.3 VVM (air volume/solution volume/minute)). To ensure well mixed conditions in the reactor, magnetic stirring was used in addition to the air sparging. Tap water was circulated around the reactor to cool the reactor and control the temperature at 25 °C.

In the batch reactor, 3 UV lamps were arranged in a triangle to minimize the areas of overlap of irradiation between lamps [4]. The UV lamps used in the batch reactor experiments were the G8T5 germicidal lamps from Sankyo Denki. The intensity for a low pressure mercury lamp is reduced from the anode in the lower part of the reactor to the cathode at the upper part of the reactor. In general, the longer the lamp, the greater the exposure area is.

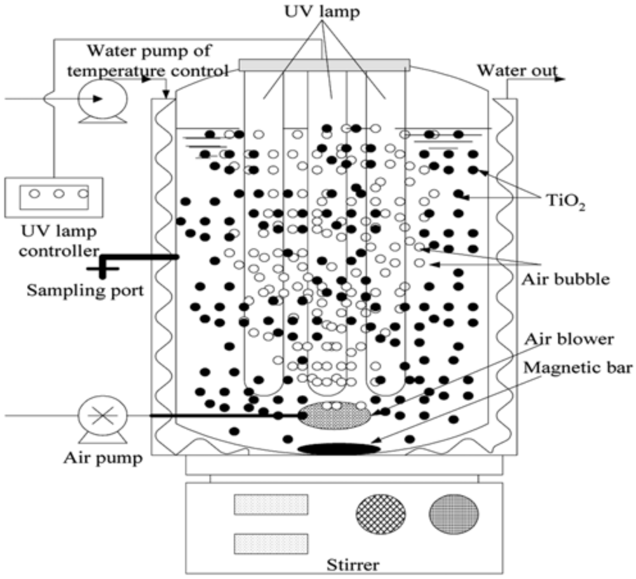

Fig. 2. Schematic of the photo-catalytic batch reactor.

2. Continuous Photo-reactor

The continuous mode photo-reactor used in this study is shown in Fig. 3. The TiO_2 and UV lamps used here are the same as those used in the batch reactor experiments. In the continuous system the gap between lamp enclosure and the walls of cylindrical reactor was 3 mm measured from the quart sleeve to the inside wall of the stainless steel reactor. The basic design conditions were adapted to ensure the following;

- In waste water treatment the flow must be turbulent (Re≥2000) [5]. A circulation of 150 mLmin^{-1} (Q2 in Fig. 3) was used to ensure turbulent conditions and to avoid the settling of TiO_2 in the photo-catalysis reactor.
- The pattern of flow through the UV reactors for disinfection should be plug flow [6].

Three stainless steel reactors with a volume of 70 mL each were used, giving a total volume of 210 mL for the continuous reactor. TiO_2 was dosed at a rate of 1.5 gL^{-1} directly into a holding tank (T1) containing 5 L of stock solution. The concentration of MM in the stock solution was 10 mgL^{-1} and it was mixed with a magnetic stirrer. One set of experiments were conducted with TiO_2 alone, while in another set of experiments a PAC dose of 0.05 gL^{-1} was added together with the TiO_2. Air sparging was also provided at the same rate as the batch reactor. The solution was then fed by a pump to a circulation tank (T2). Temperature in the recirculation tank was controlled by a thermoline in a holder tank. The solution containing TiO_2 was pumped to the continuous photo-catalytic reactor at rates of 10, 20 and 40 mLmin^{-1}. It was recirculated in the photo-catalytic reactor at a rate of 150 mLmin^{-1} (Q2 in Fig. 3) to prevent the settling of TiO_2 and PAC within the reactor. The effluent withdrawal rate (Q1 in Fig. 3) was adjusted to obtain the desired value of retention time where the retention time is equal to the volume of the photo-catalytic reactor divided by Q1. The effluent withdrawal rate in the continuous photo-reactor was set at 10, 20 and 40 mLmin^{-1} to allow retention times of 21, 10.5, 5.25 minutes, respectively.

3. Chemicals

MM 60% herbicide group B purchased from Du Pont Australia was used to prepare the synthetic water. The initial concentration of MM in the synthetic water was 10 mgL^{-1}. All solutions were prepared by using milli-q water (resistivity 18 MΩ-cm).

Titanium dioxide TiO_2-P25 A.R. grade was used as the photo-catalyst. It was purchased from Degusssa Frankfurt, Germany. It is composed of 80% anatase and 20% rutile. The BET surface area is 50±15 m^2 g^{-1}.

PAC (MD3545WB wood based powder) used in this study was purchased from James Cumming & Sons Pty Ltd., Australia. It had a mean pore diameter of 3.061 nm, a micropore volume of 0.34 cm^{3}g^{-1}, a mean diameter of 19.71 μm, a maximum ash content of 6%, a maximum moisture content of 5%, and an iodine number of 900 mgg^{-1}.

4. Analysis

MM removal in the solution was measured in terms of total organic carbon (TOC) by using the Dohrmann Phoenix 8000 UV-persulfate TOC analyzer with an autosampler. All samples were filtered through a 0.45 μm membrane prior to the TOC measurement. Thus, the TOC values obtained are, in fact, dissolved organic

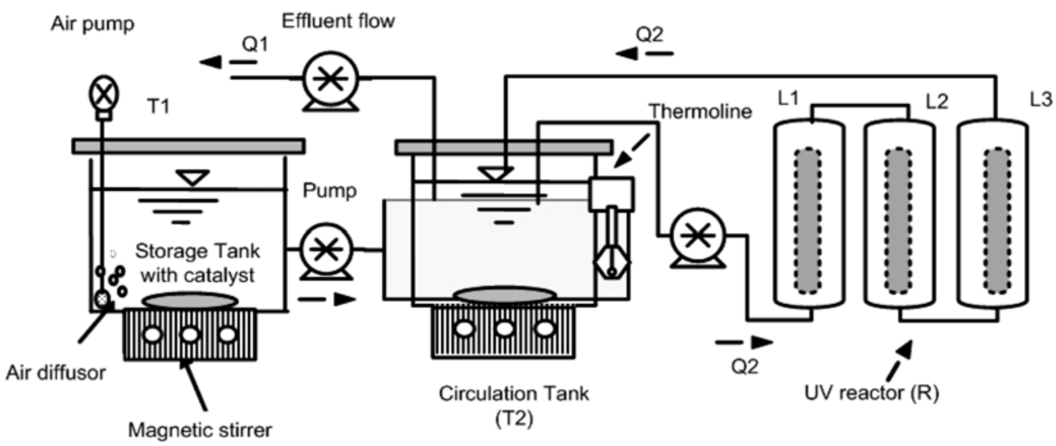

Fig. 3. Schematic of the continuous flow photo-catalytic reactor with the catalyst (T1: Mixing tank with no light source; Q1: influent and withdrawal rate; Q2: re-circulation flow; T2: re-circulation tank; R: photo-catalytic reactor unit; L1, L2, L3 are UV lamps of 8 watts each).

carbon (DOC) values.

The formation of nitrate, nitrite, and sulfate during the photocatalytic reaction was monitored by suppressed ion chromatography Dionex DX-600, which consists of GP 50 gradient pump, ED50 A detector, AS 40 automated sampler with 0.5 mL sample vials, LC 30 Chromatography Oven with a rear - loading valve, AS 14 A anion separator column and an eluent alkaline buffer containing 8 mM sodium carbonate and 10 mM sodium bicarbonate.

A Varian Gas Chromatograph 3400 (GC) equipped with a flame ionization detector FID and a DB-5 (30 m length, 0.32 mm inner diameter) column J&W, Folsom, CA was utilized for all GC analyses. The stationary phase in the column consisted of cross-linked surface bonded 5% phenyl methylpolysiloxane with a film thickness of 1ìm non-bonded. The system was operated by using helium as the carrier gas with a linear velocity of 1 $mLmin^{-1}$. The injector and detector temperatures were set at 280 °C. The only modification to the GC was the installation of a 0.75-mm diameter splitless glass inlet liner to increase the linear velocity of the flow and to leave less space for the analytes to reabsorb onto the SPME fibre. Both effects enhance desorption from the fibre.

Initial batch experiments focused on determining the time when equilibrium was established between the analytes in the stationary and aqueous phases. Triplicate solutions were extracted for periods of time ranging from 10 to 60 min of adsorption. The adsorption was assisted by using a magnetic stirrer in the 40 ml vial. The amount of adsorption was monitored after 10 min, 20 min, 30 min, 40 min, and 60 min. When the amount of adsorption did not increase any further, equilibrium was achieved. The peaks of SPME/GC chromatography after 30 minutes, 40 minutes, and 60 minutes of adsorption were similar, indicating an equilibrium time of less than 30 minutes. Therefore, 30 min of adsorption was used throughout the study. The optimization of the desorption temperature and time was investigated by considering the amount desorbed from fibers after extraction of analytes from a solution of known concentration and the subsequent carryover at a range of temperatures and time periods. The optimized conditions were to heat from 40 °C to 280 °C in the following manner. The initial column temperature was 40 °C. The temperature was increased to 100 °C at a rate of increase of 10 °C per minute and hold time for 5 minutes, then to 250 °C at a rate of increase of 30 °C per minute and hold time for 15 minutes, and finally to 280 °C at a rate of increase of 10 °C per minute and hold time for 15 minutes. The total run time was 50 minutes.

RESULTS AND DISCUSSION

Table 1. Values of C/C_o of DOC for different concentrations of TiO_2

Time (min)	Values of C/C_o of DOC for different concentrations of TiO_2			
	0.1 gL^{-1}	0.5 gL^{-1}	1.0 gL^{-1}	2 gL^{-1}
10	0.92	0.96	0.83	0.92
20	0.93	0.97	0.86	0.86
30	0.94	0.93	0.86	0.88
60	0.95	0.70	0.82	0.74
120	0.84	0.55	0.68	0.57
180	0.75	0.43	0.53	0.47
240	0.64	0.39	0.31	0.33

Table 2. Values of C/C_o of DOC for TiO_2/PAC

Time (min)	Values of C/C_o of DOC for concentrations of TiO_2/PAC			
	0.1*gL^{-1}	0.3*gL^{-1}	0.5*gL^{-1}	1*gL^{-1}
10	0.73	0.67	0.69	0.67
30	0.67	0.58	0.69	0.67
60	0.62	0.52	0.58	0.53
120	0.54	0.43	0.50	0.47
180	0.46	0.38	0.36	0.42
240	0.41	0.37	0.24	0.28

*The concentration of TiO_2 is as indicated and the concentration of PAC is 0.05 gL^{-1}

1. Batch Experiments

The results of batch experiments with TiO_2 and for PAC-TiO_2 are given in Table 1 and 2, respectively. The results are reported in terms of reduction in C/C_o at different times up to 240 minutes. C_o is the initial concentration of DOC and C is the corresponding concentration at a particular time.

Table 1 shows an initial lag stage of 30-60 min where the change in C/C_o is small. This was principally due to the time required for adsorption of MM onto the surface of TiO_2. This phenomenon was also observed by [7]. After this lag stage, the photocatalytic reaction occurred progressively. The values of C/C_o were found to decrease with TiO_2 dosage but remained relatively constant in the range of 0.5 to 2 gL^{-1} for the experimental conditions used in this study.

Experiments with different doses of TiO_2 and the addition of a small amount of PAC 0.05 gL^{-1} showed that the C/C_o reduced significantly down to 0.24 (Table 2). Furthermore, the reduction of C/C_o occurred faster with the addition of PAC. The photocatalysis process was enhanced in the presence of PAC. The PAC adsorbed intermediate by-products produced during the photo-oxidation, thereby enhancing the photocatalytic oxidation [8]. In the same manner displayed by the results of TiO_2 alone, the value of C/C_o was found to decrease initially with larger dosages of PAC-TiO_2 but remained relatively constant in the range of 0.5 to 1 gL^{-1}.

2. Batch Experiment - SPME/GC Study Characterisation of by Products

In this study, a detailed analysis with SPME/GC (solid phase micro extraction/gas chromatography) was made following batch photo-oxidation. Following 10 min of residence time in the batch reactor, the MM partitioned to smaller molecular weight compounds (or substrate) which occurred at different peak times during the GC (12.09, 14.25, 17.35, 19.61 and 20.18 minutes) (Fig. 4). In Fig. 4 the term "initial" refers to the period before photocatalysis commenced. The two initial chromatographs shown in Fig. 4 are slightly different due to the adsorption by PAC. After 5 hours of residence time in the batch reactor, some substrates degraded faster when activated carbon was used together with TiO_2 (Fig. 5). The substrate that occurred at the peak times of 19.96 and 18.32 minutes during the GC had nearly disappeared, while the peak at time 14.27 minutes was lower. Maurino et al. [9] and Vulliet et al. [7] observed that the final products of sulfonyl urea herbicides including MM were cynuric acid involving triazine moiety which hardly degrades and is harmless. Galletti et al. [10] observed MM using Varian 3400 gas chromatography (GC) equipped with Supelco SPB-5 coupled to a mass

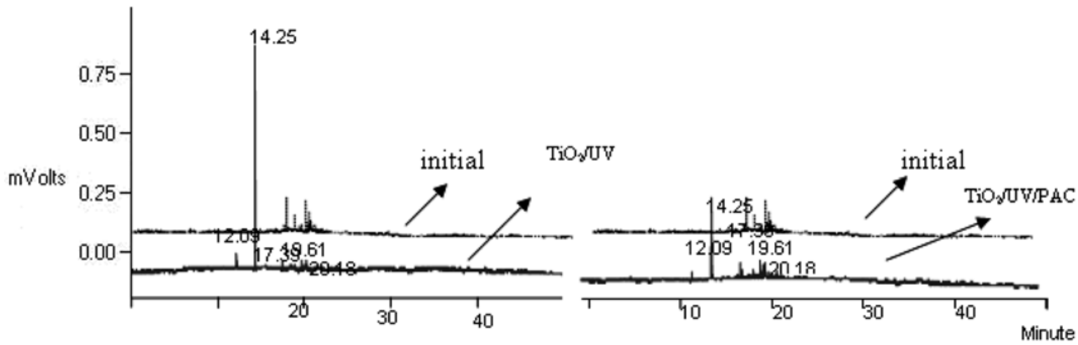

Fig. 4. 10 min SPME/GC chromatogram of MM with TiO_2 1.5 gL^{-1}.

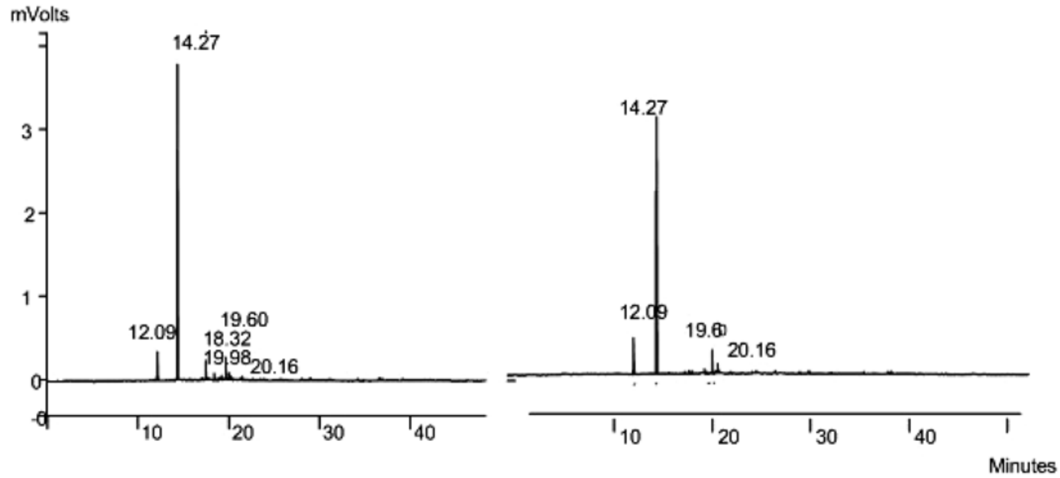

Fig. 5. 5 hours SPME/GC chromatogram of MM with TiO_2 1.5 gL^{-1}.

spectrophotometer. Their research showed the main products of MM were heterocyclic amine when the GC peak time occurred before 15 minutes (for the smaller molecular weight compound) and sulphonamide when the GC peak time occurred after 15 minute (for the larger molecular weight compound). In this study, both experiments were performed with the DB5 column of the GC by using the same mobile phase conditions as Galletti et al. [10]. The peaks occurring in these experiments were similar to Galletti et al.'s [10] results. It was assumed substrates with a peak times of 14.2 and 12.09 are heterocyclic amine. For this study, MM was partially degraded after 5 hours of residence (operation) time to substrates with GC peak times of 14.2 and 12.09 minutes. These by-products were assumed to be heterocyclic amine. If a biological metabolism process were utilized instead of photo-oxidation, much more time would be required for degradation [11].

The incomplete degradation of MM is more likely to lead to the mineralization and formation of heterocyclic amine. Some of these by-products accumulated in solution and reduced the efficiency of photo-induced degradation [7]. Inclusion of PAC increases the adsorption of by-products that otherwise will accumulate in the solution and reduce the degradation rate.

3. The Effect of Inorganic Compound in Degradation of MM

During photo-oxidation, the sulphonamide ring of the herbicide breaks down into by products such as CO_2, SO_2 and nitrogen species. In addition, NO_3^- and SO_4^{-2} of the herbicide were formed from hetero cyclic amide and sulfonamidic nitrogen of sulfonyl urea bridge, respectively, as shown in Eq. (4) [7].

$$SO_2NHCONH \rightarrow CO_2 + NO_3^- + SO_4^{2-} + SO_2 \quad (4)$$

Nitrate and nitrite ions were formed as by photo-products as shown in Fig. 6(a). The formation of NO_3^- and NO_2^- anions occurred earlier when PAC was added in the photo-oxidation (Fig. 6(b)). The presence of nitrate and nitrite in the photo-reactor can contribute to the photo-oxidation as shown in Eqs. (5), (6) and (7) [12].

$$NO_3^- + h\nu + (NO_3^-)^* \rightarrow NO_2^{\bullet} + O^{\bullet-} \quad (5)$$

$$NO_3^- + h\nu \rightarrow ONOO- \quad (6)$$

$$O^{\bullet-} + H_2O \rightarrow \bullet OH + HO^- \quad (7)$$

Similarly, SO_4^{2-} ions form during the photo-oxidation of MM. Where PAC is present in the reactor the concentration of SO_4^{2-} ions peaks earlier at approximately 50 min (Fig. 7) and thereafter is reduced in concentration. The reduction in concentration of SO_4^{2-} after 50 min may be due to a portion being adsorbed on PAC-TiO_2 surface and a portion being transformed to SO_2 gas according to the photocatalytic reaction (Eq. (4)). With TiO_2 alone, the delayed reduction in concentration of SO_4^{2-} occurring after 180 min reflects the smaller available absorbable area and active sites. Recent studies with synthetic organic compounds and herbicides of a similar nature

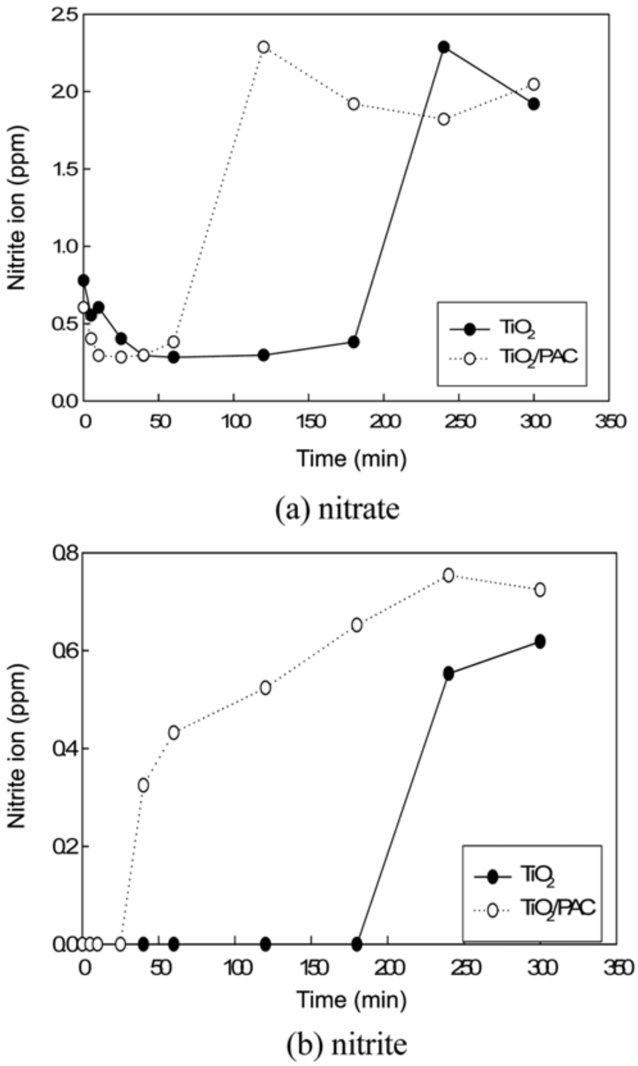

Fig. 6. Formation of (a) nitrate and (b) nitrite during the batch photocatalysis batch system (1 gL^{-1} of TiO_2 alone (solid line) and 1 gL^{-1} TiO_2 with 0.05 gL^{-1} of PAC (dotted line)).

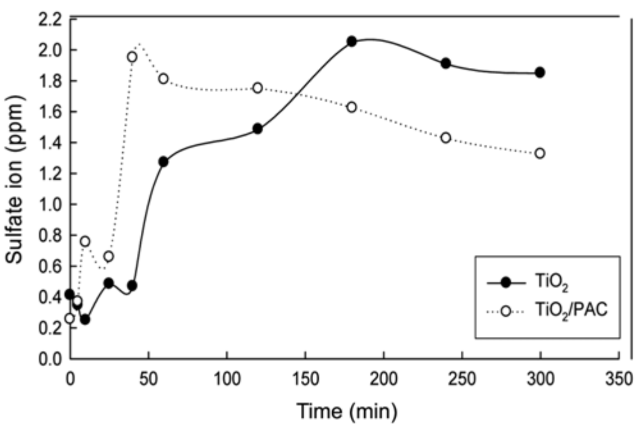

Fig. 7. Formation of sulfate anion by using TiO_2 1 gL^{-1} (solid line) and 1 gL^{-1} TiO_2 with PAC 0.05 gL^{-1} (dotted line).

showed that the presence of SO_4^{2-} ion inhibited the photo-catalytic oxidation [13,14]. The reduction in SO_4^{2-} ion means that photocatalysis is able to proceed at a faster rate. Arana et al. [15] attributed the increase in photocatalytic reaction of phenol, 4-amino phenol and salicylic acid to increased adsorption of photo-products on a larger BET surface available with activated carbon. In this study, the increase in efficiency of MM degradation is similarly attributed to the adsorption of photo-products on the larger BET surface available with TiO_2 coupled with the PAC and active sites available to react with the pollutants. This reduces the competitive adsorption on active sites of PAC-TiO_2, increasing efficiency of degradation of MM. However, complicated photo-oxidation and by-products occur during these processes, and it was very difficult to determine the real mechanism of photo-catalytic reaction on the PAC-TiO_2 surface and the role of active sites because sophisticated instruments are required to confirm this.

Table 3. DOC removal at different retention time (MM concentration=10 mgL^{-1}, TiO_2=1.5 gL^{-1}, PAC=0.05 gL^{-1})

Withdrawal rate ($mLmin^{-1}$)	Retention time (min)	% DOC removal (TiO_2/UV)	% DOC removal (TiO_2/UV/PAC)
10	21	57	86
20	10.5	57	81
40	5.25	56	78

4. Continuous Photocatalysis System

The effluent withdrawal rate in the continuous photo-reactor was set at 10, 20 and 40 $mLmin^{-1}$ to allow retention times of 21, 10.5 and 5.25 minutes, respectively (Table 3). The total volume of photo-reactor was 210 mL. In the first set of experiments TiO_2 was used alone, while in the second set 0.05 gL^{-1} of PAC was added together with the TiO_2.

In this study, the solution was mixed with the TiO_2 and PAC catalyst for 15 min in the storage tank (T1 in Fig. 3) in the absence of any light, before it was pumped to the circulation tank (T2). During this time, a small amount of DOC removal of 15% was noticed. This was due to the adsorption of MM onto the TiO_2 and/or PAC as shown during the initial periods in Fig. 8(a)-(c).

The DOC removal where TiO_2 was used alone was 56-57% (Table 3). DOC removal efficiency increased to between 78-86% when a small dose of PAC was added together with TiO_2 (Table 3). The removal efficiency at a retention time of 21 minutes (withdrawal rate of 10 $mLmin^{-1}$) was approximately 69% after 65 minutes of operation time (Fig. 8(a)). After that, there was a decrease in removal efficiency to 56% (Table 3). This decline in removal efficiency and overall low rate can be overcome by the addition of PAC as shown in Fig. 8.

All the three experiments showed an increase in removal of DOC on the order of 20-30% when PAC was used together with TiO_2 similar to the batch reactor study. Furthermore, the combined PAC-TiO_2 was able to achieve a high degradation of MM (DOC) of 78% even with at low retention time of 5.25 minutes. The removal occurs faster compared to where TiO_2 is used alone (Fig. 8). Thus, the continuous photocatalysis system yielded higher MM removal efficiency with greater flexibility.

5. DOC Removal Rates

The DOC removal for the continuous system was measured with time for different doses of TiO_2 alone and for doses of PAC-TiO_2. The concentration of DOC was plotted in the form of $\ln(C/C_0)$ a-

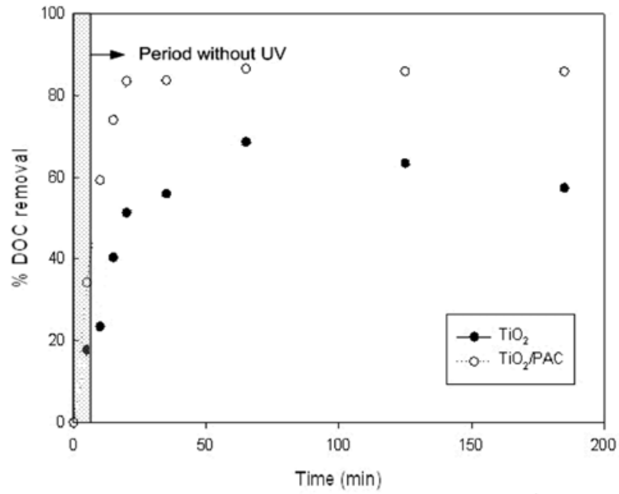

(a) withdrawal rate of 10 $mLmin^{-1}$

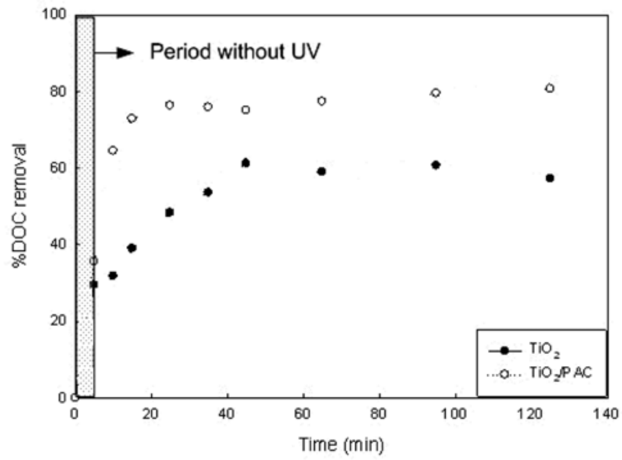

(b) withdrawal rate of 20 $mLmin^{-1}$

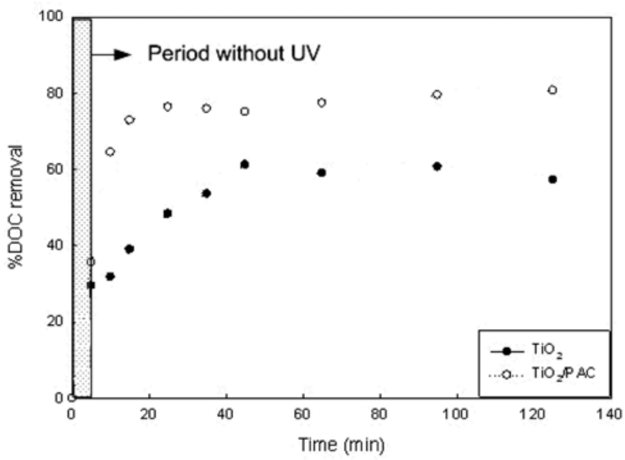

(c) withdrawal rate of 40 $mLmin^{-1}$

Fig. 8. (a)-(c) DOC removal by continuous photo-catalytic reactor.

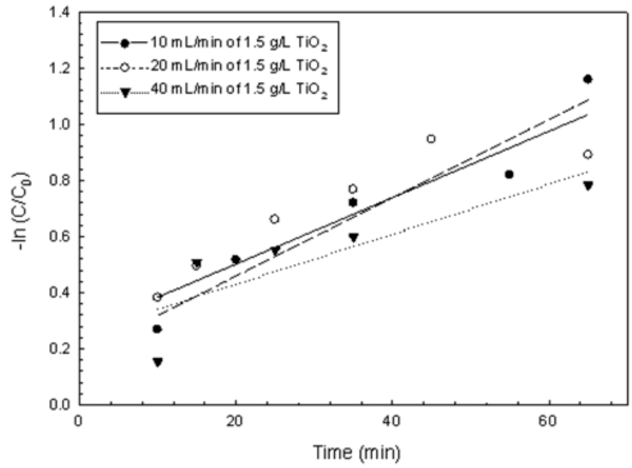

(a) 1.5 gL^{-1} of TiO_2

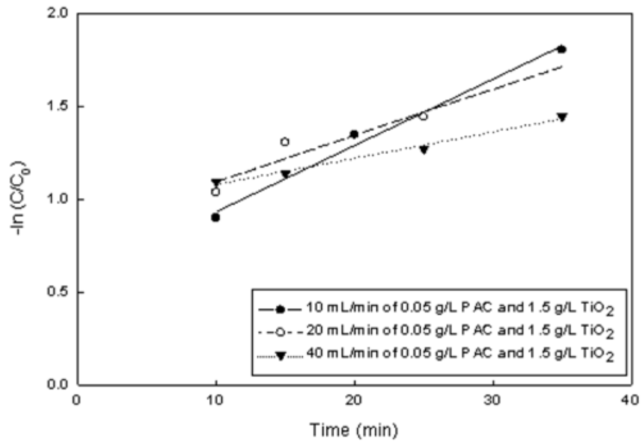

(b) 0.05 gL^{-1} PAC and 1.5 gL^{-1} of TiO_2

Fig. 9. (a)-(b) Test of pseudo first order rate constants according to Eq. (9) at different withdrawal rate and (a) with TiO_2 alone and (b) TiO_2 and 0.05 gL^{-1} PAC.

gainst the time where C_o is the initial concentration of DOC and C is the concentration at a particular time. The plot shows a near linear trend after an initial period of preliminary adsorption (Fig. 9).

The rate expression of Langmuir-Hinshelwood (L-H) (Eq. (8)) [7,16-18] is given by

$$R = -\frac{dC}{dt} = \frac{K_{Ad}kC_0}{1+K_{Ad}C_0} \quad (8)$$

where C_0=initial concentration
K_{Ad}=the adsorption coefficient
k=reaction rate constant

Integrating Eq. (8) for low initial concentration of MM gives the following equation:

$$\text{Ln}\,(C_t/C_0) = -K_{Ad}kt = k^*t \quad (9)$$

where: k^*=pseudo first order rate constant, min^{-1}, C_0 and C_t are the initial and final concentration of the MM.

From the temporal variation of DOC removal, the pseudo first order degradation rate was calculated for each dose of TiO_2 and similarly for each dose of PAC-TiO_2. The pseudo first-order constants determined and the corresponding linear regression coefficient are tabulated in Table 4. The reaction rate increased significantly with the addition of PAC (Fig. 9(b)). Comparison between ln(C/C_0) of DOC versus time for TiO_2 alone (60 minutes operation time) and for PAC-TiO_2 (35 minutes operation time) shows a higher pseudo first order rate constant in the latter. A shorter duration was used in

Table 4. Variation of pseudo first order rate constant obtained from Eq. (9) at different withdrawal rates of 1.5 gL^{-1} TiO_2

Withdrawal rate ($mLmin^{-1}$)	Retention time (min)	k* (min^{-1})	R^2
10	21	0.0168	0.87
20	10.5	0.0098	0.86
40	5.25	0.0089	0.72

Table 5. Variation of pseudo first order rate constant obtained from Eq. (9) at different withdrawal rate of 1.5 gL^{-1} TiO_2 and 0.05 gL^{-1} PAC

Withdrawal rate ($mLmin^{-1}$)	Retention time (min)	k (min^{-1})	R^2
10	21	0.0357	0.99
20	10.5	0.0251	0.87
40	5.25	0.0142	0.99

the latter because of the faster rate at which it degrades.

Tables 4 and 5 show the variation of rate constant (k^*) for the range of withdrawal rates tested. A reduction in retention time corresponds to a decrease in the pseudo first order rate constant for TiO_2 from 0.0168 min^{-1} for a retention time of 21 minutes to 0.0089 min^{-1} for retention time of 5.25 minutes (Table 3). The pseudo first order rate constants of PAC-TiO_2 increased when retention time increased from 0.0142 (5.2 minutes retention time) to 0.0357 (21 minutes retention time). However, there was also a commensurate increase in the DOC removal 78% (5.2 minute retention time) to 86% (21 minute retention time).

CONCLUSION

1. Batch Reactor

The photo-products of MM revealed higher rates of degradation of MM by using PAC-TiO_2. Higher inorganic products of MM such as NO_2^-, NO_3^- and SO_4^{2-} and small organic photo-products were produced during photo-oxidation of MM. Inorganic compounds such as SO_4^{2-} can inhibit photocatalysis. The increase in efficiency of MM degradation is attributed to the adsorption of photo-products on the larger BET surface available with PAC-TiO_2 and active sites available to react with the pollutants. This reduces the competitive adsorption on active sites of PAC-TiO_2, increasing efficiency of degradation of MM.

2. Continuous Reactor

The coupling of PAC with continuous heterogeneous photocatalysis leads to faster degradation of MM than heterogeneous photocatalysis alone. The incorporation of a small amount of PAC of 0.05 gL^{-1} with TiO_2 of 1.5 gL^{-1} led to 78% removal even with a short residence time of 5.25 minutes. The major problems of degrading herbicide and persistent organic compounds are the long period of contact time and difficult degradation. With PAC-TiO_2 continuous photocatalysis system, faster retention time and the higher removal efficiency were achieved. The system operated at a range of flows with high removal efficiency gives more flexibility for coupling with hybrid systems such as a membrane process.

ACKNOWLEDGMENT

The research is funded by Australia Research Council Discovery Grant. The first author thanks the Royal Thai Government for providing scholarship to pursue this work.

REFERENCES

1. K. M. Agbekodo, B. Legube and S. Dard, *Water Research*, **30**(11), 2535 (1996).
2. R. Molinari, M. Borgese, E. Drioli, L. Palmisano and M. Schiavello, *Catalysis Today*, **75**(1-4), 77 (2002).
3. W. Chu and C. C. Wong, *Water Research*, **38**(4), 1037 (2004).
4. W. J. Masschelein and R. G. Rice, *Ultraviolet light in water and wastewater sanitation*, Lewis Publishers, Boca Raton, Florida (2002).
5. O. K. Scheible, M. C. Casey and A. Fondran, *National technical information service*, NITS Publication 86 - 145182 (1985).
6. M. V. Thampi and C. A. Sorber, *Water Research*, **21**(7), 765 (1987).
7. E. Vulliet, C. Emmelin, J.-M. Chovelon, C. Guillard and J.-M. Herrmann, *Environ. Chem. Lett.*, **1**, 62 (2003)
8. A. Nathaporn, H. K. Shon, S. Vigneswaran and H. H. Ngo, *Water Science and Technology: Water Supply*, **6**(2), 109 (2006).
9. V. Maurino, C. Minero, E. Pelizzetti and M. Vincenti, *Colloids and Surfaces A: Physicochemical and Engineering Aspects*, **151**(1-2), 329 (1996).
10. G. C. Galletti, G. Chiavari, F. A. Mellon, and K. Parlsey, *Journal of Analytical and Applied Pyrolysis*, **21**(1-2), 239 (1991).
11. E. M. Beyer, M. J. Duffy, J. V. Hay and D. D Schlueter, *Chemistry, Degradation, and Mode of Action*, **3**, 117 (1987).
12. G. Mark, H.-G. Korth, H.-P. Schuchmann and C. von Sonntag, *Journal of Photochemistry and Photobiology A: Chemistry*, **101**(2-3), 89 (1996).
13. C. Hu, T. Yuchao, L. Lanyu, H. Zhengping and T. Hongxiao, *Journal of Chemical Technology and Biotechnology*, **79**, 247 (2004).
14. C. C. Wong and W. Chu, *Chemosphere*, **50**(8), 981 (2003).
15. J. Arana, J. M. Dona-Rodriguez, E. Tello Rendon, C. Garriga i Cabo, O. Gonzalez-Diaz, J. A. Herrera-Melian, J. Perez-Pena, G. Colon and J. A. Navio, *Applied Catalysis B: Environmental*, **44**(2), 161 (2003).
16. A. Bhattacharyya, S. Kawi and M. B. Ray, *Catalysis Today*, **98**(3), 431 (2004).
17. A. Bianco Prevot, M. Vincenti, A. Bianciotto and E. Pramauro, *Applied Catalysis B: Environmental*, **22**(2), 149 (1999).
18. Ö. E. Kartal, M. Erol and H. Oğuz, *Chemical Engineering & Technology*, **24**(6), 645 (2001).